

# Feedback Control of Morphology During III-V Semiconductor Growth by Molecular Beam Epitaxy <sup>1</sup>

Robert L. Kosut <sup>2</sup>

Russel Caffisch <sup>3</sup>

Mark Gyure <sup>4</sup>

David G. Meyer <sup>5</sup>  
Andrew Engelmann

## Abstract

This paper addresses the modeling and control of epitaxial growth of III-V semiconductor material by Molecular Beam Epitaxy. To reliably achieve the required features, processing must use fundamental understanding of the atom-by-atom assembly of these structures and careful feedback design. One problem is to develop a model relating morphology, sensor variables, and control variables. Another is to design robust feedback for achieving a desired surface morphology. A novel new model is developed and presented here as well as modifications to a previously published model. Feedback design using both models is conducted; simulation results are shown.

## 1 Introduction

The quality of quantum heterostructure devices depends crucially on the ability to control interface morphology during growth. In layer-by-layer growth mode, oscillations in the specular intensity of the reflection high energy electron diffraction (RHEED) pattern are often observed and have been correlated to the instantaneous density of steps on the surface [1, 2]. This allows for the possibility of in situ monitoring and control of surface morphology during growth. The basic processes in layer-by-layer epitaxial growth are deposition and diffusion on the surface followed by the subsequent nucleation, growth, and coalescence of islands.

The control problem here is to grow a specified number of layers while meeting a specified "roughness" criteria expressed in terms of RHEED. Figure 1 shows the MBE chamber at the HRL Laboratories which is the experimental facility for this research.

<sup>1</sup>Research supported by DARPA, Applied Computation & Mathematics Program.

<sup>2</sup>SC Solutions, Inc., 3211 Scott Blvd., Santa Clara, CA 95054, kosut@scsolutions.com

<sup>3</sup>Mathematics Department, UCLA, Los Angeles, CA 90095, caffisch@math.ucla.edu

<sup>4</sup>HRL Laboratories, 3011 Malibu Canyon Rd., Malibu, CA 90265, gyure@hrl.com

<sup>5</sup>Department of Electrical & Computer Engineering, University of Colorado, Boulder, CO 80309-0425, dgm2r@pref.colorado.edu engelman@colorado.edu

## 2 Epitaxial Growth Models

Existing models for epitaxial growth are of three types.

1. *Atomistic kinetic models* [3] describe growth through rates for various atomistic process such as diffusion of adatoms and attachment of atoms to and from steps or islands. Kinetic Monte Carlo (KMC) methods are then used to translate these rates into realistic simulations of growth.
2. *Continuum models*, including the Villain equation [4] and island dynamics models [6, 5], describe growth by a set of PDEs for various field quantities, such as adatom density  $\rho(t, x)$ , e.g.,

$$\begin{aligned}\frac{\partial \rho}{\partial t} &= F + D \nabla^2 \rho - \frac{dN}{dt} \\ \frac{dN}{dt} &= D \text{avg}_x(\rho^2)\end{aligned}\quad (1)$$

where  $t$  is time,  $x$  the planar spatial coordinate,  $F(t, x)$  is the impinging flux,  $D$  the diffusion coefficient, and  $N$  is the number of nucleated islands. Typically,  $\rho(t, x) = 0$  at the island boundaries and tracking the boundaries can be accomplished using the level set method, [6].

3. *Bulk models* describe growth through a set of scalar quantities, which are averages over the spatial domain. At present, the primary examples of a bulk model are rate equations [7], since they describe the growth through the number density  $n_k$  for islands of size  $k$ . They can describe the features of precoalescent growth of a single layer and provide qualitative information and understanding, such as scaling properties of the growth.

## 3 Morphology Variables

Two of the important morphology variables are the *step edge density*,

$$q = \text{island perimeter per unit area}$$

and the *coverage*,

$$\theta = \text{average height per lattice}$$

Theoretical and experimental studies have shown that RHEED measures  $q$  after a linear transformation. Studies are under way to determine the relation between  $q$  and the PE (photoemission) sensor. The variables that strongly effect the layer growth are the substrate temperature and adatom flux. Scaling laws show that these combine in the growth variable  $R = D/F$ , which is the inverse Peclet number and is typically very large, e.g.,  $R \geq 10^4$ . Here  $D$  is the diffusion coefficient which depends on the substrate temperature.

Figure 2 shows step edge density for constant flux  $F = .25$  monolayers/sec and varying  $D/F$  as a function of coverage,  $\theta$ , which in this case is proportional to deposition time, i.e.,  $\theta = Ft$ .

In the MBE reactor, it is not possible to rapidly change the diffusion  $D$  over the time period of typical 5-10 monolayer growth because of the slow thermal dynamics of the substrate. Hence, substrate temperature is useful as a “run-to-run” control variable. Flux, can be rapidly changed by adjusting the effusion cell cracker valves or shutters, and more slowly changed by controlling the cell temperature. Hence, the growth variable  $R = D/F$  is the effective control variable through flux. As seen in figure 2, a change in flux will effect the deposition time to achieve a desired coverage, i.e., decreasing flux increases the deposition time to reach a coverage goal and increases  $D/F$ , thereby lowering the step edge density.

If the flux,  $F$ , and diffusion,  $D$ , are constant, then for integer layers  $n = 1, 2, \dots$  such that  $\theta(t_n) = n$ ,

$$1/(t_n - t_{n-1}) = F \quad (2)$$

and many simulation runs show that the average step edge density over one layer depends only on  $R$ , that is,

$$\frac{1}{t_n - t_{n-1}} \int_{t_{n-1}}^{t_n} q(t) dt = \mathcal{A}(R) \quad (3)$$

In addition, at the  $n$ -th layer,

$$q(t_n) = Q(n, R) \quad (4)$$

In figure 3, the upper plot shows how  $q(t_n)$  varies with  $n$  and  $R$ . The lower plot shows the function  $\mathcal{A}(R)$ . Hence, for slowly varying  $(F, D)$ , we can draw the following conclusions:

- $\{q(t) \mid t_{n-1} \leq t \leq t_n\} \mapsto (F, R)$  is a *reduced growth model*
- $(F, R)$  can be estimated from measurement of  $\{q(t) \mid t_{n-1} \leq t \leq t_n\}$
- $(F, R)$  can be controlled (layer-to-layer) to obtain desired density at coverage  $n$ ,

$$q_{\text{des}} = Q(n, R_{\text{des}})$$

This leads to the following

### Morphology model

$$\begin{aligned} q(t) &= Q(\theta(t), R(t)) \\ R(t) &= D/F(t) \\ d\theta(t)/dt &= F(t) \end{aligned} \quad (5)$$

where  $Q(\theta, R)$  is an algebraic “table look-up” from *static* KMC model runs over  $(\theta, R)$ . Spline interpolation fills table as  $(\theta(t), R(t))$  evolves. Simulation studies reveal that the transient error between the above reduced model and the KMC model is negligible for slow flux variation.

For this model we report on using only the flux,  $F(t)$ , as the control. However, the flux depends on the effusion cell thermal and valve dynamics. A linear approximation is given by the following:

### Effusion cell model

$$\tau dF(t)/dt = -F(t) + F_c(t), \quad F_c(t) \geq 0$$

where  $\tau$  is the “cool-down” time constant ( $\approx 40$  sec), and  $F_c(t)$  is the heater actuation. The uncertainties in this system are:

- initial flux:  $F(0)$  is unknown because before a run begins the cell is shuttered closed, and the surface temperature builds up
- diffusion:  $D$  depends on wafer surface temperature, which is controlled, but can vary.

A detailed discussion of effusion cell modeling and control is given in [8].

## 4 Layer-to-Layer Control

Controlling the growth from layer to layer gives rise to a discrete-time controller. The strategy is to hold the flux heater command,  $F_c(t)$ , constant over each layer. Thus,

$$\begin{aligned} F_c(t) &= (F_c)_n, \quad t_{n-1} \leq t < t_n \\ &\quad \downarrow \\ F(t_n) &= a_n F(t_{n-1}) + (1 - a_n)(F_c)_n \\ a_n &= \exp\left(- (t_n - t_{n-1})/\tau\right) \end{aligned} \quad (6)$$

Using measurements of step edge density,  $q(t)$ , we compute estimates of the time to complete a layer,  $t_n$ , the average flux,  $F_n$ , and the growth variable,  $R_n$  as follows:

### growth variable estimates (via $q(t)$ )

$$\begin{aligned}\hat{t}_n &= \{t \mid q(t + \delta) - q(t) > 0, \quad q(t) - q(t - \delta) < 0\} \\ \hat{F}_n &= 1/(\hat{t}_n - \hat{t}_{n-1}) \\ \hat{R}_n &= \mathcal{A}^{-1} \left( \hat{F}_n \int_{\hat{t}_{n-1}}^{\hat{t}_n} q(t) dt \right)\end{aligned}\quad (7)$$

The parameter  $\delta$  sets the estimation error.

A control can be designed to regulate either the flux,  $F$ , or the growth variable,  $R$ . Consider, for example:

### layer-to-layer control algorithm

$$\begin{aligned}(F_c)_n &= \text{sat} \left\{ (F_c)_{n-1} + \gamma_n (E_n - a_n E_{n-1}) \right\} \\ E_n &= (F_{\text{ref}})_n - \hat{F}_n \\ (F_{\text{ref}})_n &= \begin{cases} F_{\text{des}} & \mathbf{F\text{-control}} \\ (\hat{R}_n/R_{\text{des}}) \hat{F}_n & \mathbf{R\text{-control}} \end{cases}\end{aligned}\quad (8)$$

The parameter  $\gamma_n$  sets the closed-loop bandwidth.

Simulations of the R-control under perturbations in initial flux and diffusion are shown in figure 9. The controlled system is able to almost recover performance to the ideal (unperturbed) growth. F-control was not effective in this case.

## 5 A Mass Transport Model

We now present a bulk model called the Mass Transport Model (MTM) and show some control results for this model. We modified a model presented in [9] and made the mass transport coefficients a function of temperature. Temperature translates roughly to the diffusion coefficient described earlier. The model has one state per layer,  $\theta_i$  which is the coverage on the  $i^{\text{th}}$  layer. The differential equation for each layer is

$$\begin{aligned}\frac{d}{dt}\theta_n &= J(\theta_{n-1} - \theta_n) + \mu(T)(\theta_{n+1} - \theta_{n+2})(\theta_{n-1} - \theta_n) \\ &\quad - \mu(T)(\theta_n - \theta_{n+1})(\theta_{n-2} - \theta_{n-1})\end{aligned}$$

Inputs to the model are incident flux,  $J$ , and temperature,  $T$ . The model allows for adatoms to jump down a level. The jump rate from layer  $n + 1$  to  $n$  is proportional to the product of the covered area on level  $n + 1$  and the uncovered area on level  $n$ . The mass transfer function,  $\mu$ , is modeled as a linear function of temperature,  $\mu(T) = k_0 T$ . It is assumed that the parameters  $J, T$ , and  $k_0$  are all non-negative. The initial conditions for the model are  $\theta_0 = 1.0$  and  $\theta_i = 0.0$  for  $i = 1, 2, \dots$ .

The output of the MTM is a RHEED signal. This sensor gives morphology [1, 2] information. Therefore, one control aim is to track a given, known, desirable RHEED pattern. The diffracted intensity is the square

modulus of the diffracted amplitude [9]. Simplifying assumptions can be made including that the diffracted intensity comes from top layer scatterers only and that momentum transfer parallel to substrate is zero. Under these assumptions the RHEED output of the model is

$$I = \left| \sum_{n=0}^{\infty} (\theta_n - \theta_{n+1}) (-1)^n \right|^2 \quad (9)$$

Figure 4 shows a simulation of the MTM with the linear mass transport function, constant inputs  $J = 1, T = 1$  (in normalized units), and mass transport coefficient  $k_0 = 100$ . Each subsequent curve in the top plot is the coverage of a new layer. The growth is “near perfect” in that at any time there is one layer which dominates the growth activity. The output clearly displays oscillations characteristic of a RHEED sensor pattern. Note that the output of the MTM does not exhibit the decay envelope as seen with an actual RHEED system. See Section 6 for a model that display some oscillation decay. The MTM does exhibit one important characteristic of MBE growth, and that is “recovery”. Figure 5 shows a simulation where the incident flux was shut off half way through the run. Because the MTM has diffusion terms in its dynamics, the surface smoothes and the output signal indicates that the surface has “recovered”.

Tracking of a desired trajectory is easily achieved with state feedback. The control law used was

$$u(t) = K(x_{\text{des}}(t) - x(t))$$

where  $x_{\text{des}}(t)$  is the desired state trajectory, and the feedback gains,  $K$ , is a  $2 \times n$  matrix of all ones. Figure 6 shows the states and output for the MTM when the initial condition was perturbed to  $\theta_1 = 0.5$ . Close tracking was achieved after approximately three seconds.

## 6 A Distributed Mass Transport Model

In [9], Cohen et. al. presented a model that takes into account the lateral structure in a plane. The adatoms are distributed among the layers according to the number of reactive sites available. The model, is formulated as follows. Of the  $J(\theta_n - \theta_{n+1})$  atoms arriving on top of the  $n^{\text{th}}$  layer, a fraction,  $\alpha_n$  transfer to the  $n^{\text{th}}$  and the remaining fraction,  $1 - \alpha_n$  remain on top of the  $n^{\text{th}}$  and contribute to growth of the  $n + 1$  layer coverage,  $\theta_{n+1}$ . This model does not exhibit recovery because there are no terms in its dynamic equations that allow diffusion to occur.

We modified the Cohen model in the following way. We added diffusion terms similar to the ones in the MTM. The differential equations describing the growth

for each layer are

$$\frac{d}{dt}\theta_n = \alpha_n J(\theta_n - \theta_{n+1}) + (1 - \alpha_{n-1})J(\theta_{n-1} - \theta_n) + k_0 T \theta_{n+1}(\theta_{n-1} - \theta_n) - k_0 T \theta_n(\theta_{n-2} - \theta_{n-1})$$

The distribution of incoming adatoms according to the number of reactive sites (step sites) is given by

$$\alpha_n = A \frac{d_n(\theta_n)}{d_n(\theta_n) + d_{n+1}(\theta_{n+1})}$$

where  $A$  is a constant,  $d_n(\theta_n)$  is the perimeter of the  $n^{\text{th}}$  layer and  $\alpha_n = 0$  if  $d_n = 0$  even is  $d_{n+1} = 0$ . The following assumptions are made:

- For less than half filled surface there is a fixed number of clusters, each with the same perimeter.
- For more than half filled surface, there is a fixed number of holes, each with the same perimeter.

Thus we choose,

$$d_n(\theta_n) = \begin{cases} \theta_n^{1/2}, & \text{for } \theta_n \leq 0.5 \\ (1 - \theta_n^{1/2}), & \text{for } \theta_n > 0.5 \end{cases}$$

Figure 7 shows a simulation with  $J = 1$ ,  $T = 1$ ,  $k_0 = 1.0$ , and  $A = 0.88$ . The output oscillations show decay on the upper envelope. There is no decay on the lower envelope as is observed in actual RHEED data. Figure 8 shows successful tracking results using the same control law as the one in Section 5.

## 7 Concluding Remarks

Measuring “conserved” growth properties leads to natural control. Simulations show D/F (R)-control more effective than flux (F)-control. The crude estimate of layer growth time produced some poor estimates of growth values. This can be improved. With the MTM, RHEED tracking can be achieved. Ultimately it is desirable to directly control device properties, but this needs a structures-property model.

## References

[1] J.H. Neave, B.A. Joyce, P.J. Dobson, and N. Norton *Appl. Phys.* A31:1 1983  
 [2] J.M. Van Hove, C.S. Lent, P.R. Pukite, and P.I. Cohen *J. Vac. Sci. Technol.*, B1:741, 1983  
 [3] D.D. Vvedensky. Atmospheric modeling of epitaxial growth: comparisons between lattice models and experiment. *Comp. Materials Sci.*, 6:182–187, 1996.  
 [4] J. Villain. Continuum models of crystal growth from atomic beams with and without desorption. *J. de Phys. I*, 1:19–42, 1991.

[5] M. F. Gyure, C. Ratsch, B. Merriman, R. E. Caffisch, S. Osher, J. J. Zinck and D. D. Vvedensky Level set methods for the simulation of epitaxial phenomena *Phys. Rev. E*, 58:R6927, 1998  
 [6] R.E. Caffisch, M.F. Gyure, B. Merriman, S. Osher, C. Ratsch, D. Vvedensky, and J. Zinck. Island dynamics and the level set method for epitaxial growth. *Applied Math. Letters*, 12:13–22, 1999.  
 [7] J. Venables. Rate equation approaches to thin film nucleation kinetics. *Phil. Mag.*, 27:697–738, 1973.  
 [8] M. K. Tucker and D. G. Meyer. Nonlinear modeling, identification, and feedback control design for the modern effusion cell. *J. Vac. Sci. and Technol. A.*, 16:3536–3554 Nov, 1998  
 [9] Cohen, P., G. Petrich, P. Pukite, and G. Whaley Birth-Death Models of Epitaxy I. Diffraction oscillations from low index surfaces *Surface Science* 216 (1989) 222-248.

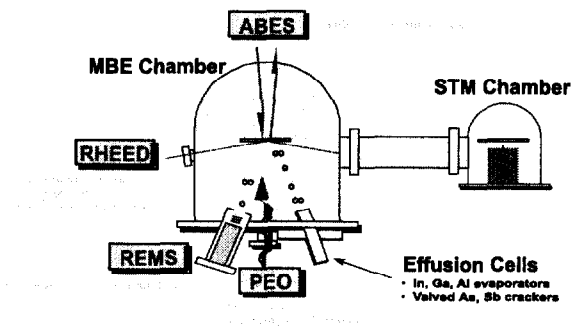


Figure 1: MBE chamber at the HRL Laboratory

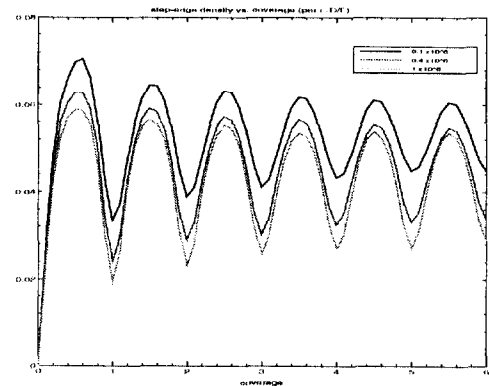
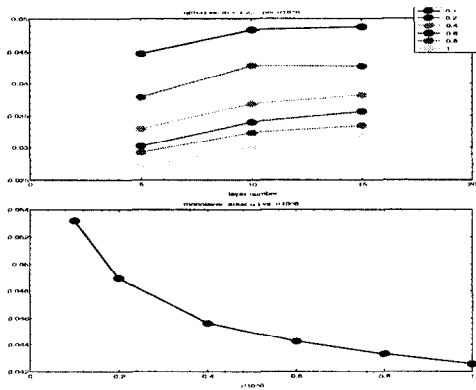
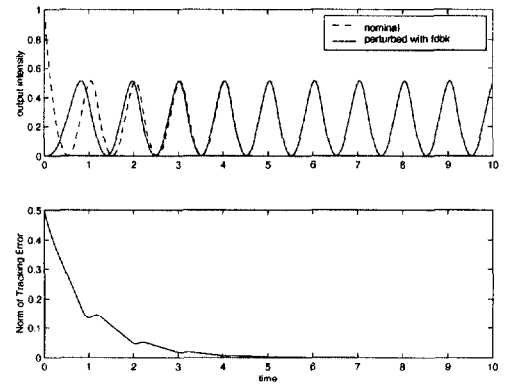


Figure 2:  $q(t)$  vs.  $\theta(t)$  for  $R = D/F \in [10^4, 10^5, 10^6]$ , flux  $F = 1$  ml/sec  $\implies \theta = Ft = t$



**Figure 3:** Upper:  $Q(n, R)$  vs.  $n = 5, 10, 15$  for  $R \in [0.1, 1] \times 10^6$ . Lower: Area under  $q$  for constant flux  $F = 1$ , over any monolayer as a function of  $R$ .



**Figure 6:** Mass Transport Model Tracking

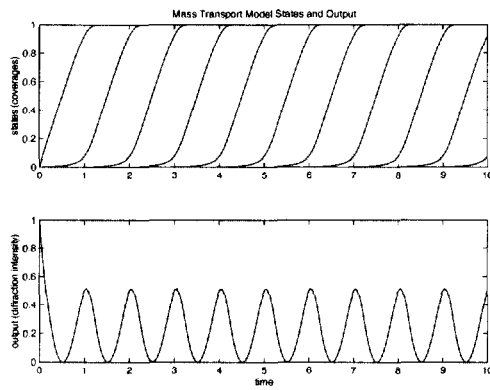


**Figure 4:** Mass Transport Model States and Output

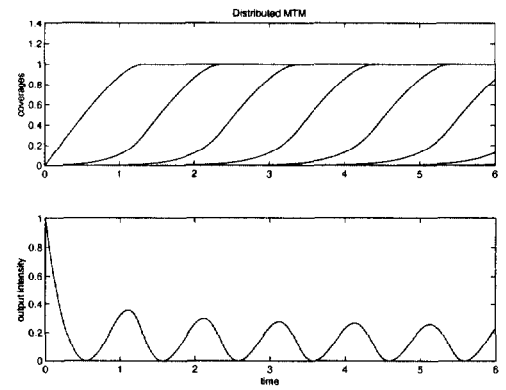


**Figure 7:** Distributed Mass Transport Model

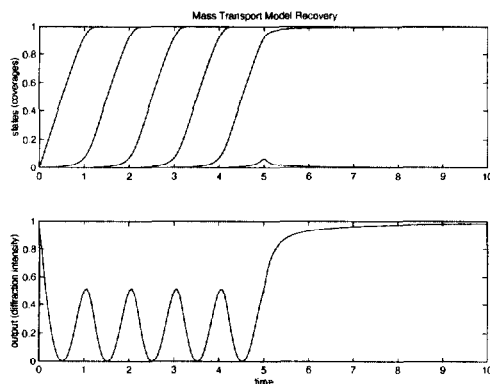


**Figure 5:** Mass Transport Model Recovery

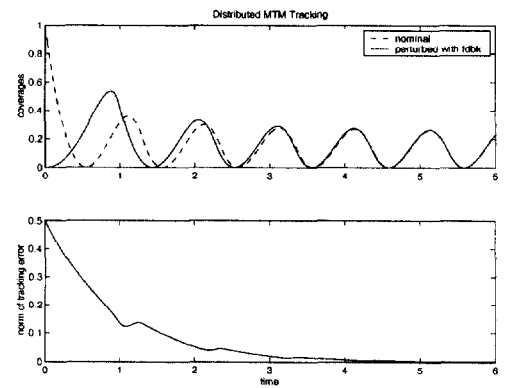
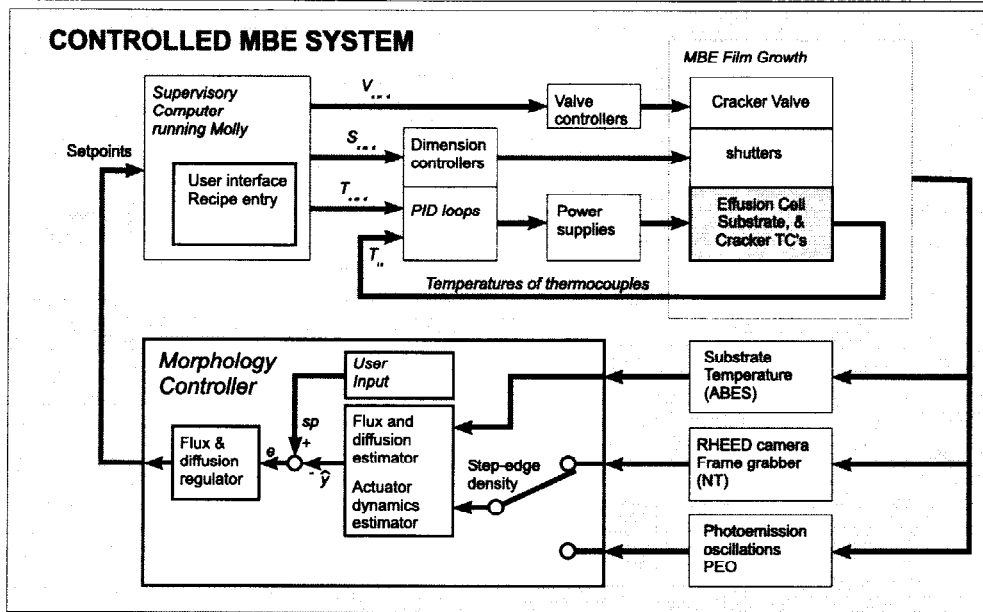
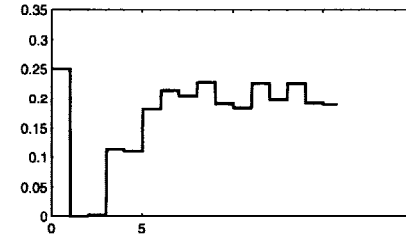


**Figure 8:** Distributed MTM Tracking

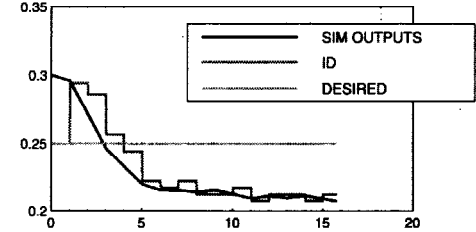
# Simulated Layer-to-Layer Morphology Control



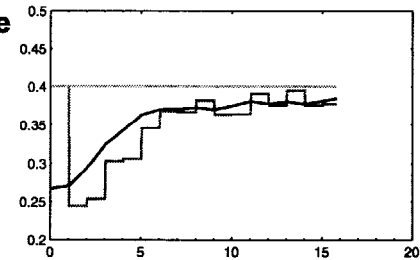
CONTROL (TEMPERATURE)



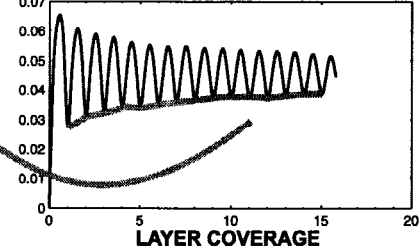
FLUX



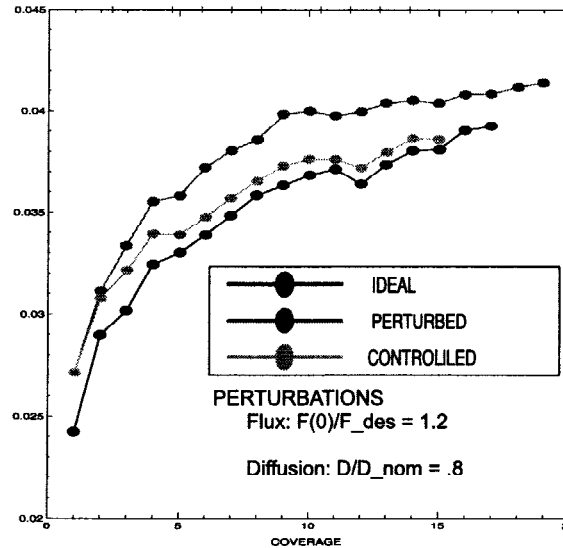
GROWTH VARIABLE (D/F)



STEP-EDGE DENSITY



Step-Edge Density at Integer Layer Coverage



## Morphology Controller

- sensor: edge density
- actuator: cell temperature
- constructs model-based estimate of growth (D/F)

Plots show simulation of controlled growth under perturbations

control recovers near ideal performance